



Design, synthesis and pharmacological evaluation of ester-based quercetin derivatives as selective vascular $K_{Ca}1.1$ channel stimulators

Gabriele Carullo^{a,b}, Amer Ahmed^c, Alfonso Trezza^b, Ottavia Spiga^b, Antonella Brizzi^b,
Simona Saponara^{c,*}, Fabio Fusi^{b,*}, Francesca Aiello^a

^a Department of Pharmacy, Health and Nutritional Sciences, DoE 2018-2022, University of Calabria, Edificio Polifunzionale, 87036 Rende (CS), Italy

^b Department of Biotechnology, Chemistry and Pharmacy, DoE 2018-2022, University of Siena, Via Aldo Moro 2, 53100 Siena, Italy

^c Department of Life Sciences, University of Siena, Via Aldo Moro 2, 53100 Siena, Italy

ARTICLE INFO

Keywords:

Ca_v1.2 channel
K_{Ca}1.1 channel
Molecular docking
Quercetin
Vasoactivity
Lipoic acid
Hypertension
Ester-based derivatives

ABSTRACT

Quercetin represents one of the most studied dietary flavonoids; it exerts a panel of pharmacological activities particularly on the cardiovascular system. Stimulation of vascular $K_{Ca}1.1$ channels contributes to its vasorelaxant activity, which is, however, counteracted in part by its concomitant stimulation of Ca_v1.2 channels. Therefore, several quercetin hybrid derivatives were designed and synthesized to produce a more selective $K_{Ca}1.1$ channel stimulator, then assessed both *in silico* and *in vitro*. All the derivatives interacted with the $K_{Ca}1.1$ channel with similar binding energy values. Among the selected derivatives, **1E** was a weak vasodilator, though displaying an interesting Ca_v1.2 channel blocking activity. The lipoyl derivatives **1F** and **3F**, though showing pharmacological and electrophysiological features similar to those of quercetin, seemed to be more effective as $K_{Ca}1.1$ channel stimulators as compared to the parent compound. The strategy pursued demonstrated how different chemical substituents on the quercetin core can change/invert its effect on Ca_v1.2 channels or enhance its $K_{Ca}1.1$ channel stimulatory activity, thus opening new avenues for the synthesis of efficacious vasorelaxant quercetin hybrids.

1. Introduction

Quercetin is a natural-occurring flavonoid that has captured the interest of scientific community, as it possesses several beneficial properties. Furthermore, it is easily isolated from a variety of food sources, such as cherries, apple, red wine, capers, and red onion [1]. Quercetin as well as many other flavonoids modulate several physiological functions, exerting anti-inflammatory [2], anti-infectious, anticancer/chemopreventive [3], neuroprotective, wound regenerating [4,5], blood glucose lowering [6,7] and anti-hypertensive/vasorelaxant activities [8]. Focusing on cardiovascular diseases, clinical studies demonstrate that Corvitin® (a water-soluble form of quercetin for i.v. use) has beneficial effects on clinical forms of ischemic heart disease, including myocardial infarction. The antiarrhythmic action of Corvitin may be the result of its membrane-stabilizing action, as well as of the improvement of intracardiac hemodynamics due to the reduction of myocardial stress.

Moreover, Corvitin stabilizes the necrotic zone and reduces the mass of the necrotized myocardium [9]. Administration of quercetin (either before the onset of ischemia or during whole reperfusion) improves the recovery of cardiac function after global ischemia and reperfusion [10]. Quercetin supplementation for 14 days protects rats from isoproterenol-induced acute myocardial injury: cardioprotective effects include a significant attenuation of oxidative stress and inflammation, preservation of heart architecture, along with downregulation of calpain expression. Moreover, rats treated with quercetin do not show any sign of progression of experimental autoimmune myocarditis to dilated cardiomyopathy [11]. This was ascribed to the decrease of myocardial levels of endoplasmic reticulum stress and fibrosis markers via modulation of endothelin-1/MAPK signalling cascade.

Various mechanisms underpin the cardiovascular properties of quercetin. In particular, quercetin is capable, along with many other flavonoids, to stimulate $K_{Ca}1.1$ channels [12], activated by membrane

Abbreviations: CHCl₃, chloroform; CMC, 1-cyclohexyl-3-(2-morpholinoethyl)carbodiimide; DCM, dichloromethane; DMF, *N,N*-dimethylformamide; DMSO, dimethyl sulphoxide; HOBt, *N*-hydroxybenzotriazole; HPLC, high-pressure liquid chromatography; I_{KCa1.1}, $K_{Ca}1.1$ channel currents; IP₃, inositol trisphosphate; MAPK, mitogen activated protein kinase; MeOH, methanol; PKA, protein kinase A; PKG, protein kinase G; TEA, tetraethylammonium; TLC, thin-layer chromatography.

* Corresponding authors.

E-mail addresses: simona.saponara@unisi.it (S. Saponara), fabio.fusi@unisi.it (F. Fusi).

<https://doi.org/10.1016/j.bioorg.2020.104404>

Received 3 September 2020; Received in revised form 8 October 2020; Accepted 19 October 2020

Available online 22 October 2020

0045-2068/© 2020 Elsevier Inc. All rights reserved.

depolarization and/or changes in the sub-plasmalemmal Ca^{2+} concentration, and controlled by numerous intracellular chemical ligands and kinases.

Noticeably a reduced $\text{K}_{\text{Ca}1.1}$ channel function and/or expression, leading to vasoconstriction, has been associated to a number of pathological conditions including hypertension, type 2 diabetes mellitus, ischemia/reperfusion or brain injury, haemorrhagic shock and atherosclerosis [13]. Therefore, $\text{K}_{\text{Ca}1.1}$ channels represent important targets for therapeutic intervention [14].

Quercetin causes coronary vasodilation due, at least in part, to a H_2O_2 -mediated increase of the iberiotoxin-sensitive $\text{K}_{\text{Ca}1.1}$ channel currents ($I_{\text{KCa}1.1}$) [15]. This effect has been ascribed to the pro-oxidant activity of the flavonoid that manifests under certain experimental conditions. Furthermore, quercetin increases the frequency of spontaneous transient $I_{\text{KCa}1.1}$, which are triggered by Ca^{2+} sparks, and hyperpolarizes the cell membrane, thus potentiating a fundamental feedback mechanism in vascular function that contrasts membrane depolarization and vasoconstriction. It is noteworthy that this effect on $I_{\text{KCa}1.1}$ is already significant at low concentrations, similar to those observed in human plasma after the ingestion of quercetin-rich foods [16]. Quercetin stimulates vascular $I_{\text{KCa}1.1}$ with a mechanism that seems to be tissue-specific. In fact, in the rat tail main artery this effect partly occurs via a protein kinase G (PKG)-mediated, catalase-independent mechanism [17]. Additionally, in this tissue the flavonoid decreases both the frequency and the amplitude of spontaneous transient $I_{\text{KCa}1.1}$ by reducing the amount of Ca^{2+} releasable from the sarcoplasmic reticulum [18].

Among Ca^{2+} channels, Ca_V channels constitute the predominant Ca^{2+} influx route in vascular smooth muscle cells and support several functions in the cardiovascular system: action potential generation and pacemaking activity, cardiac inotropism and atrial excitability, arterial myogenic tone and vascular resistance. Surprisingly, though behaving as a vasodilator *in vitro* as well as *in vivo*, quercetin stimulates $\text{Ca}_\text{V}1.2$ current in clonal rat pituitary GH4C1 cells, via cAMP-induced activation of protein kinase A (PKA) [19], in guinea-pig gut [20] and in rat vascular smooth muscle cells, where stimulation is rather specific, since quercetin does not affect the co-expressed $\text{Ca}_\text{V}3.1$ channels [21–23]. However, $\text{Ca}_\text{V}1.2$ channel stimulation by quercetin causes an influx of extracellular Ca^{2+} that is not sufficient to overcome its myorelaxing activity. This hypothesis is corroborated by the observation that maximal activation of $\text{Ca}_\text{V}1.2$ channels by Bay K 8644 (i.e. larger influx of extracellular Ca^{2+} as

compared to that measured with quercetin alone) indeed prevails over quercetin-induced myorelaxation, thus causing smooth muscle contraction [24]. Finally, low μM concentrations of the flavonoid are capable to counteract $\text{Ca}_\text{V}1.2$ channel stimulation operated by Bay K 8644 [25]. As this effect on $\text{Ca}_\text{V}1.2$ channels can anyhow affect its vasorelaxant activity, the aim of the present work was to design quercetin derivatives as more selective modulators of $\text{K}_{\text{Ca}1.1}$ channels, somehow devoid of the stimulatory activity on or even blocking $\text{Ca}_\text{V}1.2$ channels, in order to produce novel selective vasorelaxing agents. New hybrid compounds, ester-derivatives were thus designed choosing acyl donors of natural source, because of their known vasodilating properties [26] and structural similarities with other $\text{K}_{\text{Ca}1.1}$ channel ligands such as MTx, SKA 31, and DIBAC₄(3) (Fig. 1) [27,28]. Synthesized compounds were assessed for their vascular and ion channel modulating activity in intact tissue and isolated myocytes, while analyzing in depth their interaction with the channel protein *in silico*. Findings indicate future strategies to improve quercetin selectivity towards $\text{K}_{\text{Ca}1.1}$ channels as compared to $\text{Ca}_\text{V}1.2$ channels.

2. Results and discussion

2.1. *In silico* screening

Semi-synthetic hybrids were designed, by using different acyl donors (Fig. 1), derived from natural sources, with reported vasoactive properties, as just demonstrated [26,29].

Twenty-four quercetin derivatives (see Table 1 Supporting information) were designed according to the key chemically reactive centers of the molecule, namely C-4', C-3 and C-7 [30,31]. To select the best leads among the series an *in silico* docking approach was followed. Firstly, a blind docking was performed for each compound to identify a potential binding region on the $\text{K}_{\text{Ca}1.1}$ channel. All the molecules localized, with high frequency, in a region proximal to the S6 segment (Fig. 2A). A rational docking simulation was then carried out to obtain the most accurate binding mode for each ligand. Interestingly, all derivatives located in the same binding pocket, assuming a comparable binding pose (Fig. 2 B-C). Their binding affinity for the target was high, ranging from $-10.2 \text{ kcal mol}^{-1}$ (1E) to $-7.6 \text{ kcal mol}^{-1}$ (3F) (see Table 1 Supporting information). A careful analysis of the ΔG values suggested that, in general, the C-3 substitution gave rise to molecules with lower

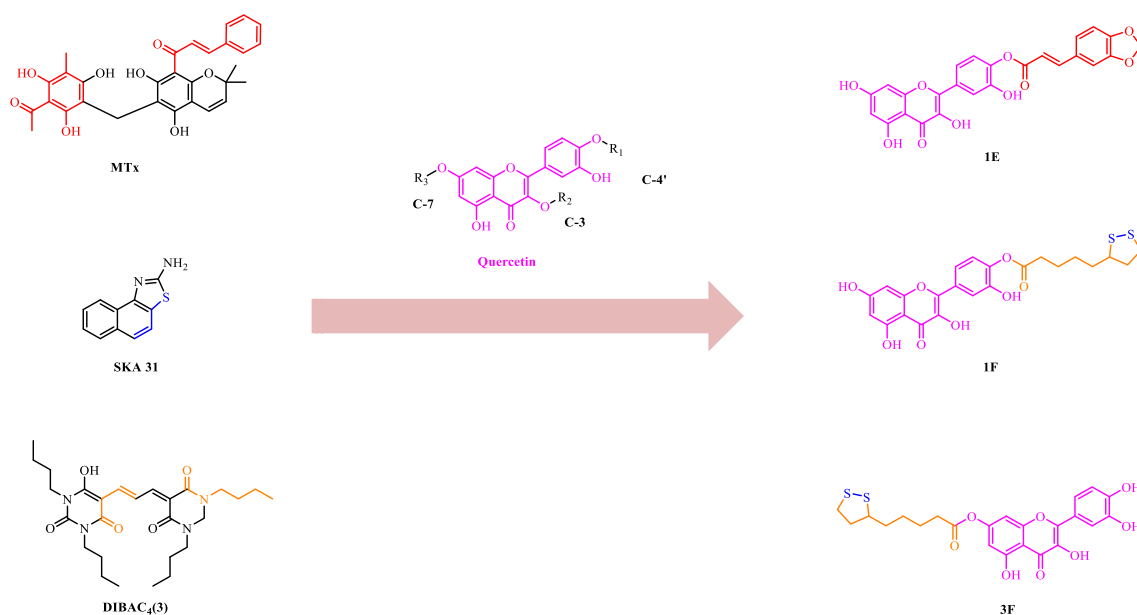


Fig. 1. Design of new quercetin derivatives as selective $\text{K}_{\text{Ca}1.1}$ channel stimulators starting from quercetin and already described $\text{K}_{\text{Ca}1.1}$ channel stimulators (MTx, SKA31, and DIBAC₄(3)).

Table 1

K_{Ca}1.1 channel-compound interaction network summary. The consensus binding residues are highlighted in bold.

Compound	Hydrophobic interaction	Hydrogen bond	π -Stacking	π -Cationic	ΔG (kcal mol ⁻¹)
1E	Arg-395, Tyr-402 , Lys-458, Phe-461 , Glu-465	Lys-300 , Tyr-398 , Tyr-402 , Glu-454, Phe-466, Tyr-467	Tyr-398	Lys-458	-10.2
1F	Arg-395, Tyr-402 , Lys-458, Phe-461	Lys-300 , Asn-394, Tyr-398 , Tyr-402 , Lys-458, Val-464, Phe-466	Tyr-398 , Phe-461	Lys-458	-9.3
3F	Lys-397, Tyr-402 , Lys-458, Phe-461 , Glu-465	Lys-300 , Ser-383, Tyr-398 , Tyr-402 , Glu-454	Tyr-398 , Phe-461		-7.6

ΔG values as compared to the C-7 and C-4' substituted ones. Therefore, the two compounds with the highest and lowest ΔG values, respectively, were selected as the most representative of the series. Among the intermediate ΔG values, a C-4' substituted derivative (**1F**) was preferred to attain also SAR indications (Table 1).

The interaction network analysis indicated that the three ligands formed different bonds within the binding pocket (Fig. 3 A-C), only a few interactions being conserved. In particular, all compounds shared three hydrophobic interactions with Tyr-402, Lys-458, and Phe-461, three hydrogen bonds with Lys-300, Tyr-398, and Tyr-402, and a π -stacking interaction with Tyr-398. The region identified as the potential binding pocket of quercetin derivatives plays a key role in K_{Ca}1.1 channel activation [32].

In fact, Gessner *et al.* [28] showed through *in vitro* mutagenesis that residues located in this region, particularly Tyr-402, are crucial both for the activation of the channel and for the modulator binding. Therefore, the hydrogen bond formed by all derivatives with Tyr-402 may trigger a conformational change of S6/RCK linker, inducing K_{Ca}1.1 channel stimulation. Noticeably, the three hydrophobic interactions with Tyr-402, Lys-458, and Phe-461, the other two hydrogen bonds with Lys-300 and Tyr-398, and the π -stacking interaction with Tyr-398, might represent novel consensus binding sites for K_{Ca}1.1 channel modulators.

In silico results showed that the three derivatives were able to bind with high affinity inside the K_{Ca}1.1 channel binding pocket located in the S6/RCK linker. Furthermore, the K_{Ca}1.1 channel-compound interaction network suggested that the potential mechanism of action of the ligands might be based on the hydrogen bond formed with Tyr-402.

2.2. Chemistry

According to these computational data, three derivatives named **1E**, **1F**, and **3F** were synthesized by simple chemical procedures (Scheme 1).

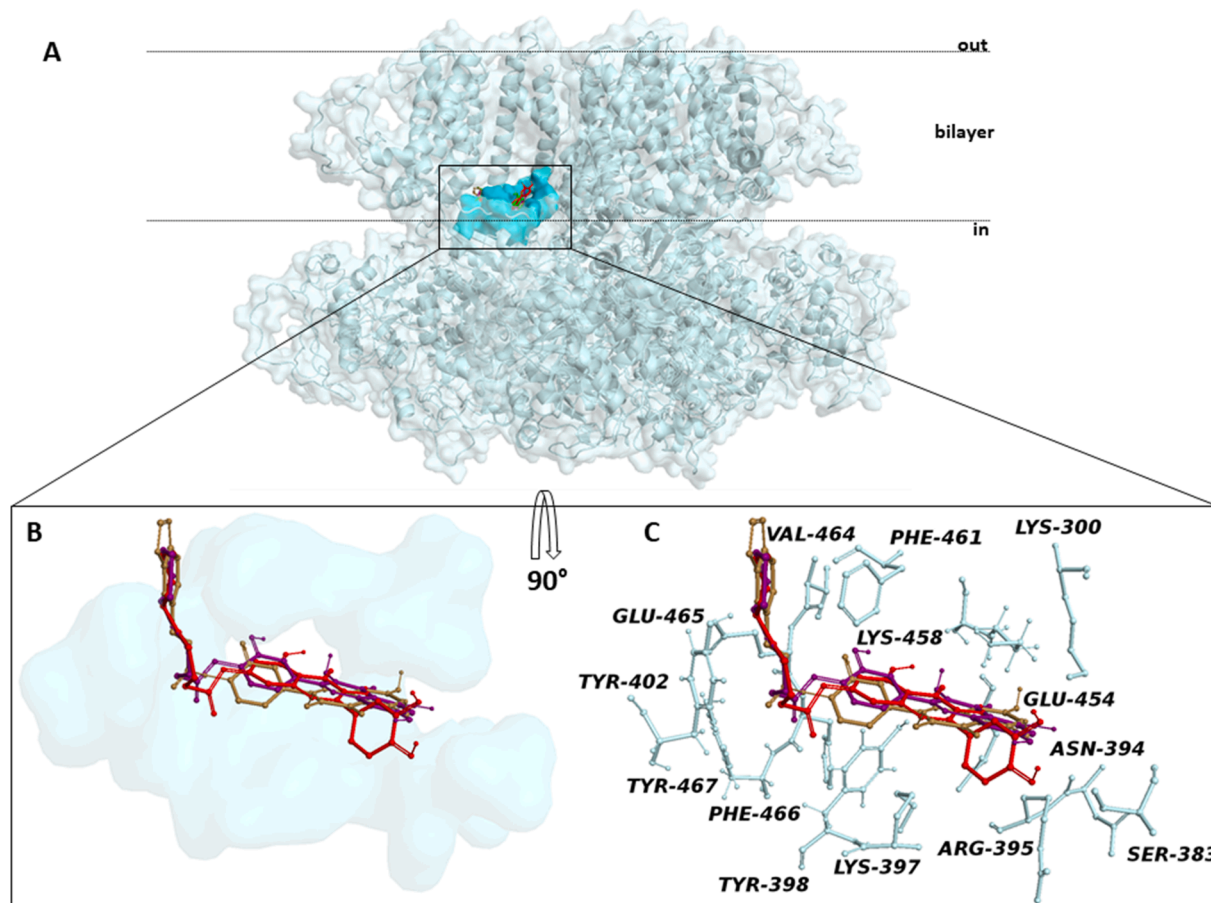


Fig. 2. K_{Ca}1.1 channel-compound docked poses overview. (A) The K_{Ca}1.1 channel protein is represented as a transparent cyan surface cartoon while the binding pocket is shown in cyan surface. Compounds **1E**, **1F**, and **3F** are depicted as gold, purple, and magenta sticks and balls. The membrane bilayer is delimited by two black dotted lines (B,C) Enlarged and twisted view of docked poses of compounds into the K_{Ca}1.1 channel binding pocket. (For interpretation of the references to colour in this figure legend, the reader is referred to the web version of this article.)

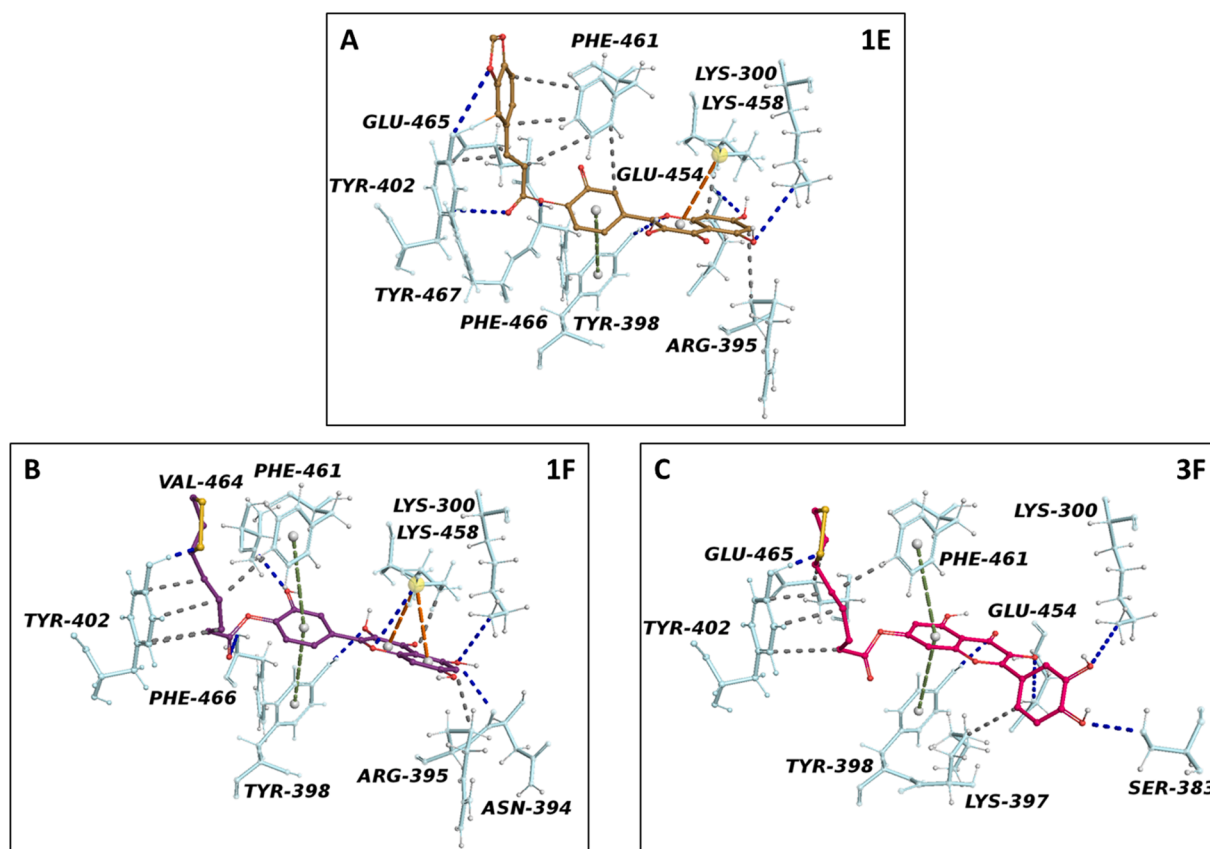
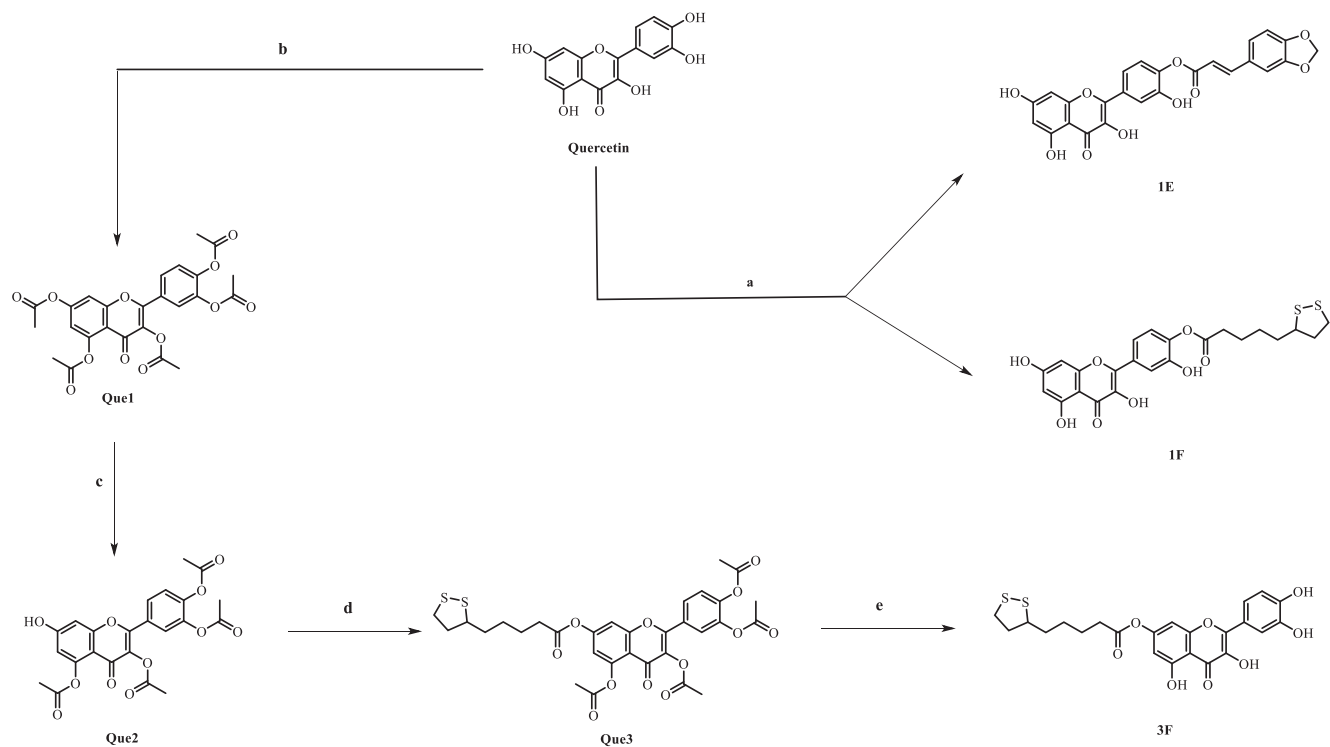


Fig. 3. $K_{Ca}1.1$ channel binding residues-ligand interaction network. (A) 1E, (B) 1F, and (C) 3F are displayed in gold, purple, and magenta balls and sticks, whereas the $K_{Ca}1.1$ channel binding residues are in cyan. Hydrophobic interactions, hydrogen bonds, π -stacking, and π -cationic interactions are depicted as grey, blue, green, and orange dotted lines. (For interpretation of the references to colour in this figure legend, the reader is referred to the web version of this article.)



Scheme 1. Synthesis of the selected quercetin derivatives as $K_{Ca}1.1$ channel stimulators. Reagents and conditions: a) 3,4-(methylenedioxy)cinnamic acid (for 1E), α -lipoic acid (for 1F), HOBT, CMC, DCM, DMF, 0 °C, 15 min, then rt, 24 h; b) acetic anhydride, pyridine, reflux, 5 h; c) imidazole, DCM, -15 °C, then rt, 2 h; d) α -lipoic acid, HOBT, CMC, DCM, DMF, 0 °C, 15 min, then rt, 24 h; e) 6 N aqueous HCl, CH_3CN .

1E and **1F** were synthesized through a Steglich reaction performed by using 1-cyclohexyl-3-(2-morpholinoethyl)carbodiimide (CMC), and *N*-hydroxybenzotriazole (HOBt): **1E** and **1F** were thus obtained in acceptable yield (32% and 46%, respectively). The NMR analysis, identified only C-4' esters. Anything else, if present, was considered as a side product.

A different approach was followed for the synthesis of **3F**, because the OH in C-7 position is the third in order of reactivity of quercetin core [7]. Firstly, quercetin was converted to its penta-acetylated derivative **Que1**, which was selectively deacetylated in C-7 position with imidazole. The product **Que2** was then subjected to Steglich conditions to obtain the ester **Que3**, which was converted to the final compound **3F** in acidic conditions. **1E**, **1F**, and **3F** were then assessed for their vascular activity.

2.3. Pharmacological evaluation

In a first series of experiments, **1E**, **1F**, and **3F** were tested on rings pre-contracted with high KCl, which depolarizes the membrane, thus causing $\text{Ca}_v1.2$ channels to open. Quercetin was also assessed as positive control. In rings depolarized with 25 mM KCl, **1F**, **3F**, and quercetin caused a concentration dependent relaxation of equal potencies and efficacy (Fig. 4A). However, **1E** was only partially effective, showing a relaxant effect of $27.5 \pm 6.3\%$ ($n = 4$). In preparations depolarized with 60 mM KCl, **1F** and quercetin showed a vasorelaxant activity superimposable to that recorded on 25 mM KCl-stimulated rings (Fig. 4B). The spasmolytic activity of **3F** was significantly greater than that of the parent compound quercetin. Furthermore, **1E** efficacy was further reduced. High KCl-induced contraction is essentially due to the opening

of $\text{Ca}_v1.2$ channels and the ensuing Ca^{2+} influx from the extracellular space. In particular, the two KCl concentrations employed here (namely 25 mM and 60 mM) represented standardized experimental settings to detect K^+ channel openers and Ca^{2+} antagonists, respectively [33]. In fact, the former should be more efficacious on 25 mM KCl-induced contraction whereas the latter on that induced by 60 mM KCl. As no significant differences were observed between the two experimental settings, it can be hypothesized that the vasorelaxant activity of quercetin and its derivatives cannot be ascribed only to a $\text{Ca}_v1.2$ channel blockade or to a $\text{K}_{\text{Ca}1.1}$ channel stimulation. Of note two findings: the weak myorelaxant activity displayed by **1E** and the higher efficacy of **3F** as compared to quercetin in rings depolarized with 60 mM KCl.

The effects of **1E**, **1F**, and **3F** were further investigated on rings pre-contracted with the α -adrenergic receptor agonist phenylephrine. Fig. 4C shows that **3F** and quercetin relaxed aorta ring preparations in a concentration-dependent manner, with a similar pattern of potency and efficacy. **1F** was less active, whereas **1E** spasmolytic activity accounted for a mere 10% relaxation at the maximal concentration assessed.

Phenylephrine-induced contraction is the result of Ca^{2+} release from the sarcoplasmic reticulum triggered by inositol trisphosphate (IP_3) and Ca^{2+} influx from the extracellular space through receptor-, store-operated, and $\text{Ca}_v1.2$ channels [34]. Therefore, quercetin and **3F**, **1F** to a lesser extent, but not **1E**, likely affect one or more of these pathways leading to vasorelaxation.

Taken together, aorta ring findings suggest that the introduction of a lipoyl moiety in C-7 position leaves unaltered or even improves quercetin vasorelaxant activity, whereas that in C-4' position does not change or slightly reduces it. The latter observation is further supported by the marked reduction of vasorelaxant activity characterizing **1E** that

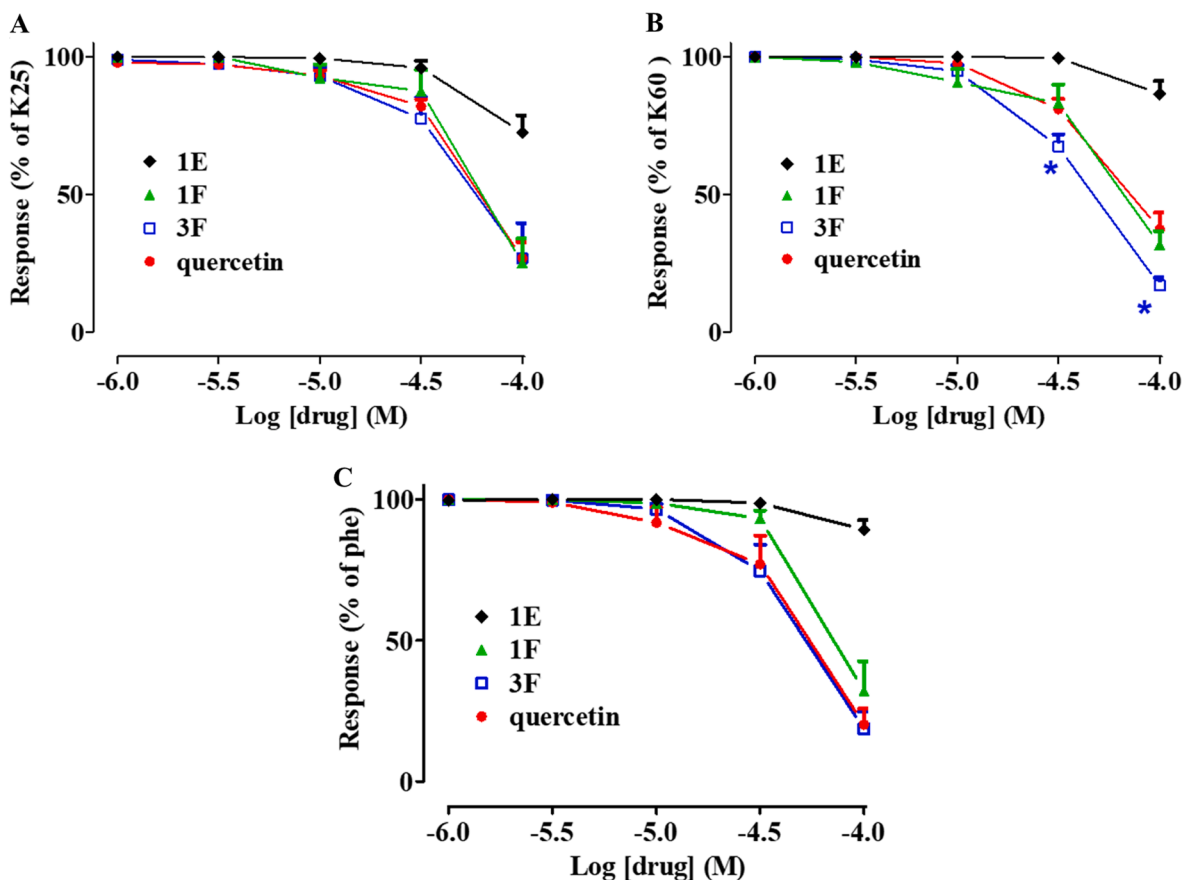


Fig. 4. Effects of quercetin and its derivatives on rat aorta rings. Endothelium-deprived rings were pre-contracted with (A) 25 mM KCl (K25), (B) 60 mM KCl (K60), or (C) 0.3 μM phenylephrine (phe). On the plateau of the contraction, cumulative concentrations of quercetin, **1E**, **1F** or **3F** were added. On the ordinate axis muscle tension is reported as percentage of the initial tone evoked by either KCl or phenylephrine. Data points represent mean \pm s.e.m. ($n = 4-6$). * $P < 0.05$ vs. quercetin, Student's *t* test for unpaired samples.

bears a 3,4-methylenedioxcynnamoyl moiety in C-4' position.

These results prompted us to investigate the effects of the most and the less active vasorelaxants, i.e. **3F** and **1E**, respectively, on Ba^{2+} current through $\text{Ca}_v1.2$ channels ($I_{\text{Ba}1.2}$), which play a fundamental role in the regulation of vascular smooth muscle tone.

Fig. 5 shows recordings of the inward current elicited with a clamp pulse to 0 mV from a V_h of -50 mV under control conditions and after the addition of cumulative concentrations of **1E** (panel A) and **3F** (panel B). Surprisingly, **1E** inhibited peak $I_{\text{Ba}1.2}$ in a concentration-dependent manner, inhibition being around 40% at the maximal concentration assessed (100 μM). In contrast, **3F** showed a biphasic behaviour, first stimulating with a pEC_{50} value of 5.58 ± 0.07 M ($n = 5$) and then inhibiting $I_{\text{Ba}1.2}$. Under similar experimental conditions quercetin stimulated $I_{\text{Ba}1.2}$ with a pEC_{50} value of 5.09 M [21]. These findings demonstrate that quercetin derivatization with a 3,4-methylenedioxcynnamoyl moiety as occurred in **1E** gave rise to a novel agent not only deprived of $\text{Ca}_v1.2$ channel stimulating activity, but also possessing a moderate but significant Ca^{2+} antagonist effect. On the contrary, **3F**, bearing a lipoyl moiety in C-7 position, did not affect the $I_{\text{Ba}1.2}$ stimulatory activity of the parent flavonoid.

$I_{\text{Ba}1.2}$ evoked at 0 mV from a V_h of -50 mV activated and then declined with a time course that could be fitted by a monoexponential function. The two derivatives slowed significantly the τ of activation, though with different concentration-dependent patterns, bell-shaped for **3F**, exponential-like for **1E** (Fig. 6). These behaviours paralleled those observed on current amplitude. **3F**, at 10 μM concentration, slowed significantly also the τ of inactivation.

Under similar experimental conditions also quercetin slowed down significantly the τ of activation without affecting that of inactivation [21]. Taken together, these findings demonstrate that the two different derivatizations did not modify the capability of the parent compound to slow down the transition of $\text{Ca}_v1.2$ channels from the closed to the open state or, in some other way, to modify the gating mechanism. Furthermore, the presence of a lipoyl moiety in C-7 (**3F**) gave rise to a derivative that slowed down $\text{Ca}_v1.2$ channel inactivation during the depolarizing pulse.

Given the weak vasorelaxant activity of **1E**, the present work focused on **3F** and its analogue **1F**, which showed myorelaxant effects comparable to those of quercetin. The final aim was to verify whether the lipoyl moiety and its position might affect quercetin stimulation of $\text{K}_{\text{Ca}1.1}$ channels. Fig. 7 (left column) shows the current-voltage relationships of $I_{\text{KCa}1.1}$ elicited with clamp pulses in the range -20 mV and 70 mV from a V_h of -40 mV, under control conditions and after the cumulative addition of 10–30 μM **1F** (panel A), or 3–10 μM **3F** (panel B). The two derivatives stimulated current amplitude in a concentration-dependent manner with a similar efficacy.

In fact at 70 mV, 10 μM **1F** or **3F** increased $I_{\text{KCa}1.1}$ amplitude by 53.4% and 68.3%, respectively. These results are in line with that

observed with quercetin under similar experimental conditions (i.e. 78.6%) [21].

Fig. 7 (right column) shows the time course of current amplitude stimulation induced by the two derivatives. No significant differences were observed in the kinetics of stimulation. Furthermore, **1F** and **3F**, at the maximal concentration assessed, did not modify the kinetics of channel activation measured at the depolarizing pulses to 70 mV (Fig. 7). Under control conditions, τ of activation were 44.69 ± 5.23 ms and 40.95 ± 4.64 ms ($n = 5$). Similar values were recorded in the presence of 30 μM **1F** (50.41 ± 8.19 ms) or 10 μM **3F** (37.12 ± 4.72 ms; $P > 0.05$).

3. Conclusions

The present findings suggest that the introduction of a lipoyl moiety in quercetin structure only marginally affected its $I_{\text{KCa}1.1}$ stimulatory activity, particularly when present in C-7 position. Furthermore, the OH group in C-7 and C-4' positions does not seem crucial to this activity. The design strategy pursued along with the *in silico* analysis gave rise to quercetin derivatives either endowed of Ca^{2+} antagonist features (compound **1E**) or displaying $\text{K}_{\text{Ca}1.1}$ channel stimulatory activity and vasorelaxant effects comparable to that of the parent compound (compounds **1F** and **3F**). These findings open new avenues for the derivatization of quercetin to improve its beneficial vascular activity.

4. Experimental section

4.1. Docking studies

The homology 3D model of the *Rattus Norvegicus* $\text{K}_{\text{Ca}1.1}$ channel was used as previously described [12]. The chemical structures of the designed compounds (Table 1) were drawn using Chemdraw software, and optimized prior to the docking procedure by using the Dock Prep. To study the binding mode of compounds to the channel, a docking simulation was performed carrying out a flexible side chain protocol with AutoDock/VinaXB [35]. The pdbqt files of ligands were obtained by Open Babel tool v. 2.4.1 [36], while pdbqt format of the receptor was created by AutoDock Vina v. 1.1.2 tools [37]. The Protein–Ligand Interaction Profiler (PLIP) generated multiple ligand–protein interaction maps [38]. PyMOL v. 2.2 was used as molecular graphics system (The PyMOL Molecular Graphics System, Version 2.2 Schrödinger, LLC).

4.2. General chemical informations

Commercially available reagents purchased from Merck (Milan, Italy) were used without further purification, and all solvents were of HPLC quality. Reactions under nitrogen atmosphere were performed in oven- or flame-dried glassware and anhydrous solvents, and then

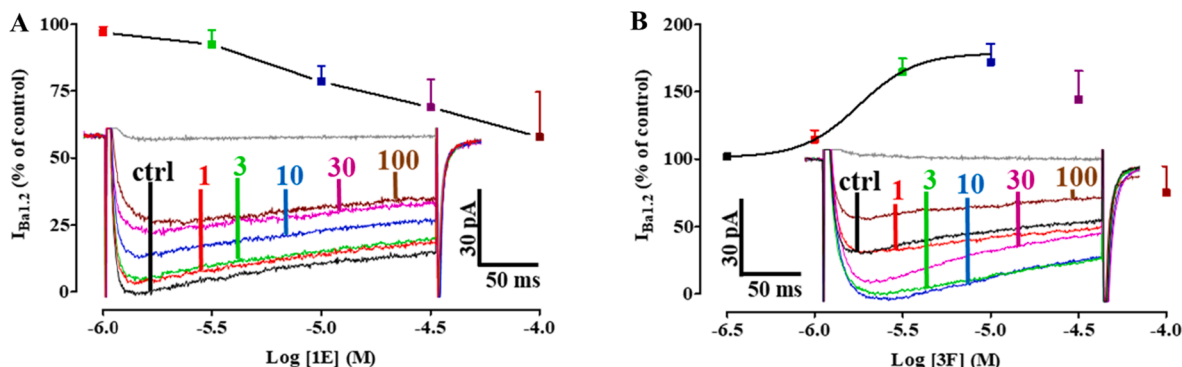


Fig. 5. Effects of **1E** and **3F** on $I_{\text{Ba}1.2}$ recorded in rat tail artery myocytes. Concentration-dependent effect of (A) **1E** and (B) **3F**. On the ordinate scale $I_{\text{Ba}1.2}$ amplitude is reported as percentage of that recorded just before drug addition. Data points are means \pm s.e.m. ($n = 4-5$). Insets: current traces (averaged from 5 cells) recorded with a clamp pulse to 0 mV from a V_h of -50 mV in the absence (ctrl) or presence of various concentrations (μM) of quercetin derivatives.

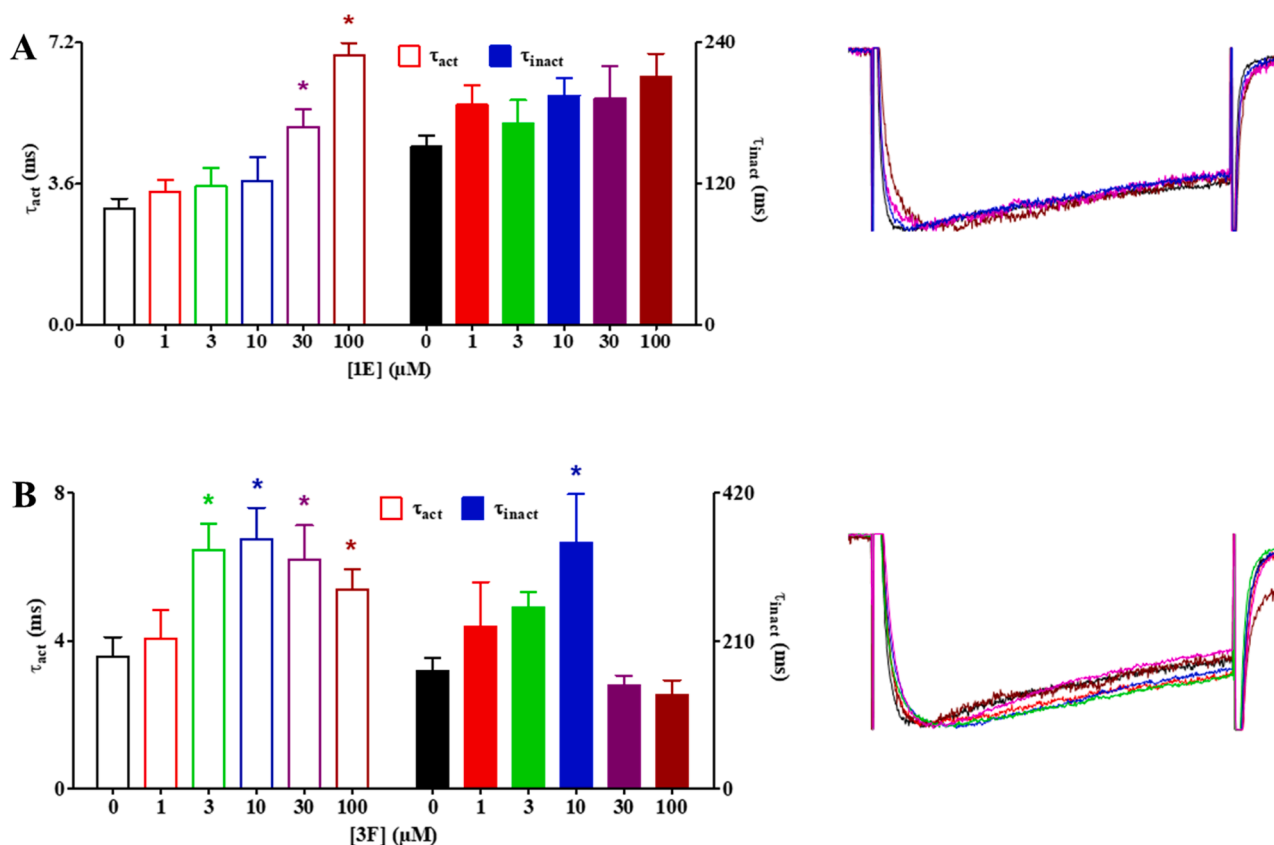


Fig. 6. Effects of **1E** and **3F** on $I_{Ba1.2}$ kinetics recorded in rat tail artery myocytes. Concentration-dependent effect of (A) **1E** and (B) **3F** on time constant of current activation (τ_{act} ; open columns) or inactivation (τ_{inact} ; closed columns). Columns are means \pm s.e.m. ($n = 5$) * $P < 0.05$, repeated measures ANOVA and Dunnett's post-test. Right: current traces (averaged from 5 cells) sized so that the peak amplitude of the traces in presence of the drug matched that of the control.

monitored by thin-layer chromatography (TLC) Merck 60 F254 silica plates. Analytical TLC was conducted on Merck aluminum sheets covered with silica (C60). The plates were either visualized under UV-light (254 nm) or stained by dipping in a developing agent followed by heating with $KMnO_4$ [3 g in water (300 mL) along with K_2CO_3 (20 g) and 5% aqueous NaOH (5 mL)]. Flash column chromatography was performed using silica gel 60 (0.040–0.063 mm). The synthesized compounds were characterized by 1H NMR, ^{13}C NMR (Bruker Advance operating at 300 MHz) and melting point (m.p.) when applicable. Unless otherwise stated, all NMR spectra were recorded at 25 °C. The chemical shifts (δ) are reported in parts per million (ppm) and the coupling constants (J) in Hz. For spectra recorded in $CDCl_3$, signal positions were measured relative to the signal for $CHCl_3$ (7.26 ppm for 1H NMR and 77.16 ppm for ^{13}C NMR). For spectra recorded in $DMSO-d_6$, signal positions were measured relative to the signal for $DMSO$ (δ 2.50 ppm for 1H NMR and 39.52 ppm for ^{13}C NMR). For spectra recorded in acetone- d_6 , signal positions were measured relative to the signal for acetone (δ 2.60 ppm for 1H NMR and 30.0 and 206 ppm for ^{13}C NMR). Anhydrous quercetin (99%, HPLC), CMC, HOBT, α -lipoic acid, and acetic anhydride were purchased from Merck (Milan, Italy).

4.2.1. Procedure a): Synthesis of compounds **1E** and **1F**

A solution of carboxylic acid (1 equiv.), quercetin (1 equiv.), and HOBT (1.2 equiv.) in anhydrous DCM/DMF (65:35) (5 mL) was cooled at 0 °C and stirred under nitrogen atmosphere for 15 min as previously described [39]. Thereafter, a solution of CMC (1.5 equiv.) in dry DCM (3.5 mL) was added dropwise. The mixture was stirred at rt for 24 h, washed twice with a 5% aqueous $NaHCO_3$ solution and finally once with brine. The collected organic layers, dried on anhydrous Na_2SO_4 , were concentrated and the pure compound obtained after flash-column chromatography (eluent DCM/MeOH 15/1).

4.2.1.1. 2-hydroxy-4-(3,5,7-trihydroxy-4-oxo-4H-chromen-2-yl)phenyl (E)-3-(benzo[d][1,3]dioxol-5-yl)acrylate 1E. Yellow resin, 32% yield. 1H NMR ($DMSO-d_6$): δ 8.10–7.90 (m, 3H), 7.72 (d, 1H, $J = 4.6$ Hz), 7.66–7.59 (m, 1H), 7.52–7.41 (m, 2H), 7.35 (d, 1H, $J = 4.6$ Hz), 6.90 (dd, 2H, $J = 3.0, 15.0$ Hz), 6.10 (s, 2H). ^{13}C NMR ($DMSO-d_6$): δ 176.2, 166.5, 164.0, 162.0, 159.0, 152.2, 148.0 (x3C), 139.9, 136.4, 127.0, 126.1, 123.0, 122.4, 121.6, 116.1 (x2C), 115.3, 108.0, 105.9, 104.0, 100.2, 98.3, 94.1. Anal. Calcd for $C_{25}H_{16}O_{10}$: C, 63.03; H, 3.39. Found: C, 62.89; H, 3.27.

4.2.1.2. 2-hydroxy-4-(3,5,7-trihydroxy-4-oxo-4H-chromen-2-yl)phenyl 5-(1,2-dithiolan-3-yl)pentanoate 1F. Yellow resin, 46% yield. 1H NMR ($DMSO-d_6$): δ 7.59 (s, 1H), 7.50–7.40 (m, 1H), 6.80–6.70 (m, 1H), 6.34 (s, 1H), 6.10 (s, 1H), 3.60–3.50 (m, 2H), 3.20–3.01 (m, 2H), 2.50–2.30 (m, 1H), 2.10–1.80 (m, 1H) 1.70–1.40 (m, 7H). ^{13}C NMR ($DMSO-d_6$): δ 176.1, 172.0, 166.4, 161.8, 158.8, 150.8, 146.9, 139.2, 136.5, 127.0, 124.0, 120.8, 114.3, 104.5, 98.3, 94.0, 61.4, 45.2, 43.3, 39.6, 38.2, 29.6, 24.6. Anal. Calcd for $C_{23}H_{22}O_8S_2$: C, 56.32; H, 4.52; S, 13.07. Found: C, 55.62; H, 5.01; S, 12.08.

4.2.2. Procedure b): Synthesis of 2-(3,4-diacetoxyphenyl)-4-oxo-4H-chromene-3,5,7-triyl triacetate **Que1**

Quercetin (1 equiv.), acetic anhydride (20 equiv.), and pyridine (15 mL) were stirred at reflux for 5 h. Then, a mixture of ice-water (50 g) was added. The resulting precipitate was filtered and washed with cold EtOAc to obtain **Que1**. White solid, 79% yield. Spectroscopic data are in agreement with those previously reported [40].

4.2.3. Procedure c): Synthesis of 4-(3,5-diacetoxy-7-hydroxy-4-oxo-4H-chromen-2-yl)-1,2-phenylene diacetate **Que2**

A solution of imidazole (2 equiv.) in DCM (5 mL) was added

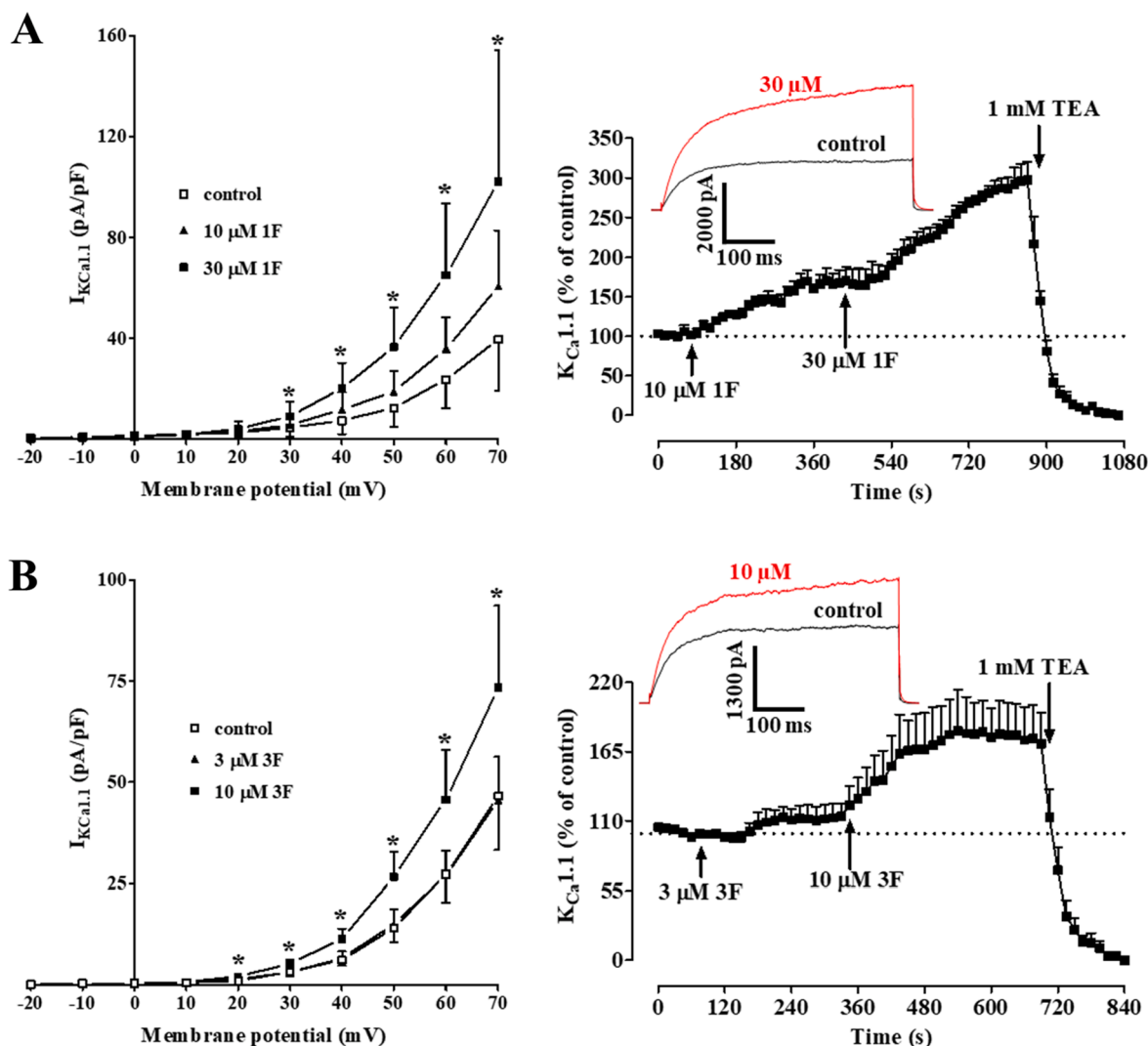


Fig. 7. Effects of 1F and 3F on $I_{KCa1.1}$ recorded in rat tail artery myocytes. Left: concentration-dependent effect of (A) 1F and (B) 3F. On the ordinate scale $I_{KCa1.1}$ amplitude is reported in pA/pF. Data points are means \pm s.e.m. ($n = 5$). * $P < 0.05$, repeated measures ANOVA and Dunnett's post-test. Right: time-course of current stimulation caused by (A) 1F and (B) 3F. On the ordinate scale $I_{KCa1.1}$ is reported as percentage of that recorded just before the addition of the first concentration of the derivative. The effect of 1 mM TEA, which blocked $I_{KCa1.1}$, is also shown. Insets: current traces (averaged from 5 cells) recorded in the absence (control) or presence of (A) 30 μ M 1F, or (B) 10 μ M 3F. $I_{KCa1.1}$ was elicited with a clamp pulse to 70 mV from a V_h of -40 mV, delivered every 10 s.

dropwise to a solution of **Que1** (1 equiv.) in DCM (10 mL) at -15 °C in an ice/acetone bath. The mixture was allowed to warm to rt and stirred for 2 h. The reaction mixture was diluted in DCM (50 mL) and washed with 3 M aqueous HCl (3×50 mL). The organic layer was then dried over anhydrous Na_2SO_4 and filtered. The solvent was evaporated under reduced pressure. The resulting residue was purified through flash-column chromatography (eluent: $CHCl_3/MeOH$, 97/3). White solid, 87% yield. Spectroscopic data are in agreement with those previously reported [40].

4.2.4. Procedure d): Synthesis of 7-((5-(1,2-dithiolan-3-yl) pentanoyl)oxy)-2-(3,4-diacetoxyphenyl)-4-oxo-4H-chromene-3,5-diyl diacetate **Que3**

This product was obtained with the same procedure used for compounds **1E** and **1F**. Yellow resin, 78% yield. 1H NMR ($CDCl_3$): δ 7.80–7.60 (m, 1H), 7.40–7.32 (m, 2H), 6.92–6.86 (m, 2H), 3.30–3.10 (m, 1H), 2.80–2.30 (m, 15H), 2.01–1.40 (m, 9H). ^{13}C NMR ($CDCl_3$): δ 178.6, 169.3, 167.9 (x 3C), 167.8, 154.2, 150.3, 144.3, 126.4, 125.0, 124.0, 123.8, 122.3, 115.5, 114.1, 107.9, 56.2, 40.2, 38.5, 34.5, 33.7, 33.5, 28.6, 24.5, 24.3, 21.1, 21.0, 20.7, 20.6, 20.5.

4.2.5. Procedure e): Synthesis of 2-(3,4-dihydroxyphenyl)-3,5-dihydroxy-4-oxo-4H-chromen-7-yl 5-(1,2-dithiolan-3-yl)pentanoate **3F**

Que3 (1 equiv.) was added to CH_3CN (20 mL) and 6 N aqueous HCl (10 mL). The resulting solution was stirred at reflux for 1.5 h. Then EtOAc (100 mL) and water (100 mL) were added. The organic layer was washed with 3 N aqueous HCl (3×100 mL), dried over anhydrous Na_2SO_4 and filtered. The solvent was evaporated under reduced pressure. **3F** was obtained after precipitation of the residue with DCM. Yellow resin, 80% yield. 1H NMR (Acetone- d_6): δ 12.30 (bs, OH-(C5), 1H), 9.80 (bs, OH-(C4'), 1H), 8.70 (bs, OH-(C3'), 1H), 8.40 (bs, OH-(C3), 1H), 7.83 (s, 1H), 7.70–7.50 (m, 1H), 7.01–6.90 (m, 1H), 6.51 (s, 1H), 6.28 (s, 1H), 3.60–3.50 (m, 2H), 3.20–3.01 (m, 2H), 2.50–2.30 (m, 1H), 2.10–1.80 (m, 1H) 1.70–1.40 (m, 7H). ^{13}C NMR (Acetone- d_6): δ 180.8, 169.2, 166.5, 161.9, 152.6, 151.2, 150.0, 146.9, 141.0, 136.0, 128.0, 125.7, 120.4, 120.0, 108.4, 103.4, 98.7, 61.4, 45.2, 43.3, 39.6, 38.2, 29.6. Anal. Calcd for $C_{23}H_{22}O_8S_2$: C, 56.32; H, 4.52; S, 13.07. Found: C, 56.20; H, 4.32.

4.3. Pharmacological analysis

4.3.1. Animals

All experimental protocols were approved by the Animal Care and Ethics Committee of the University of Siena and Italian Department of Health (7DF-19.N.TBT) and carried out in accordance to the European Union Guidelines for the Care and the Use of Laboratory Animals (European Union Directive 2010/63/EU). Male Wistar rats, weighing 325–450 g were purchased from Charles River Italia (Calco, Italy) and maintained in an animal house facility at 25 ± 1 °C and 12:12 h dark-light cycle with free access to standard chow diet and water. Animals were anaesthetized with an isoflurane (4%) and O₂ gas mixture by using Fluovac (Harvard Apparatus, Holliston, Massachusetts, USA), decapitated and exsanguinated. The thoracic aorta and tail (cleaned of skin) were immediately removed and placed in physiological solution [namely modified Krebs-Henseleit solution (KHS)] or external solution (see below for composition), respectively.

4.3.2. Cell isolation procedure

The tail main artery was dissected free of its connective tissue and smooth muscle cells were freshly isolated under the following conditions. A 5-mm long piece of artery was incubated at 37 °C for 40–45 min in 2 mL of 0.1 mM Ca²⁺ external solution (in mM: 130 NaCl, 5.6 KCl, 10 HEPES, 20 glucose, 1.2 MgCl₂, and 5 Na-pyruvate; pH 7.4) containing 20 mM taurine, which replaced an equimolar amount of NaCl, 1.35 mg mL⁻¹ collagenase (type XI), 1 mg mL⁻¹ soybean trypsin inhibitor, and 1 mg mL⁻¹ bovine serum albumin. This solution was gently bubbled with a 95% O₂-5% CO₂ gas mixture to stir the enzyme solution and cells isolated as previously described [41]. Cells stored in 0.05 mM Ca²⁺ external solution containing 20 mM taurine and 0.5 mg mL⁻¹ bovine serum albumin at 4 °C under air were used for experiments within two days after isolation [42].

4.3.3. Whole-cell patch clamp recordings

An Axopatch 200B patch-clamp amplifier (Molecular Devices Corporation, Sunnyvale, CA, USA) was used to generate and apply voltage pulses to the clamped cells and record the corresponding membrane currents. At the beginning of each experiment, the junction potential between the pipette and bath solution was electronically adjusted to zero. Current signals, after compensation for whole-cell capacitance and series resistance (between 70% and 75%), were low-pass filtered at 1 kHz and digitized at 3 kHz prior to being stored on the computer hard disk. Electrophysiological responses were tested at room temperature (20–22 °C).

4.3.4. I_{Ba1.2} recording

Cells were continuously superfused with external solution containing 0.1 mM Ca²⁺ and 30 mM tetraethylammonium (TEA) using a peristaltic pump (LKB 2132, Bromma, Sweden) at a flow rate of 400 μL min⁻¹. The conventional whole-cell patch-clamp method was employed to voltage clamp smooth muscle cells. Recording electrodes were pulled from borosilicate glass capillaries (WPI, Berlin, Germany) and fire-polished to obtain a pipette resistance of 2–5 MΩ when filled with internal solution. The internal solution (pCa 8.4) consisted of (in mM): 100 CsCl, 10 HEPES, 11 EGTA, 2 MgCl₂, 1 CaCl₂, 5 Na-pyruvate, 5 succinic acid, 5 oxaloacetic acid, 3 Na₂ATP, and 5 phosphocreatine; the pH was adjusted to 7.4 with CsOH. Ba²⁺ current through Cav1.2 channels (I_{Ba1.2}) recorded in an external solution containing 30 mM TEA and 5 mM Ba²⁺, was elicited with 250 ms clamp pulses (0.067 Hz) to 0 mV from a V_h of -50 mV. Data were collected once the current amplitude had been stabilized (usually 7–10 min after the whole-cell configuration had been obtained) [43]. Under these conditions, the current did not run down during the following 40 min [44,45] K⁺ currents were blocked with 30 mM TEA in the external solution and Cs⁺ in the internal solution. Current values were corrected for leakage and residual outward currents using 10 μM nifedipine, which completely blocked I_{Ba1.2}. The osmolarity of the 30

mM TEA- and 5 mM Ba²⁺-containing external solution (320 mOsmol) and that of the internal solution (290 mOsmol) were measured with an osmometer (Osmostat OM 6020, Menarini Diagnostics, Florence, Italy).

4.3.5. I_{KCa1.1} current measurement

I_{KCa1.1} (registration period 500 ms) was measured over a range of test potentials from -20 to 70 mV from a V_h of -40 mV. This V_h limited the contribution of K_V channels to the overall whole-cell current. Data were collected once the current amplitude had been stabilized (usually 8–10 min after the whole-cell configuration had been obtained) [46]. I_{KCa1.1} current did not run down during the following 20–30 min under the present experimental conditions. The external solution for I_{KCa1.1} recordings contained (in mM): 145 NaCl, 6 KCl, 10 glucose, 10 HEPES, 5 Na-pyruvate, 1.2 MgCl₂, 0.1 CaCl₂, 0.003 nifedipine (pH 7.4). The internal solution contained (in mM): 90 KCl, 10 NaCl, 10 HEPES, 10 EGTA, 1 MgCl₂, 6.41 CaCl₂ (pCa 7.0); pH 7.4. The osmolarity of the external and internal solutions were 310 mosmol and 265 mosmol, respectively. The current-voltage relationships were calculated on the basis of the values recorded during the last 200 ms of each test pulse (leakage corrected). I_{KCa1.1} was isolated from other currents as well as corrected for leakage using 1 mM TEA, a specific blocker of K_{Ca1.1} channels [16].

4.4. Functional experiments

4.4.1. Preparation of rat aorta rings

The thoracic aorta was immediately removed, gently cleaned of adherent tissues, and cut into 3.0-mm wide rings. The endothelium was removed by gently rubbing the lumen of the ring with forceps tip. Rings were mounted in organ baths between two parallel L-shaped stainless steel hooks, one fixed in place and the other connected to an isometric transducer. Rings were allowed to equilibrate for 60 min in a modified KHS (composition in mM: 118 NaCl; 4.75 KCl; 1.19 KH₂PO₄; 1.19 MgSO₄; 25 NaHCO₃; 11.5 glucose; 2.5 CaCl₂; gassed with a 95% O₂-5% CO₂ gas mixture to create a pH of 7.4) under a passive tension of 1 g [47]. Isometric tension was recorded using a digital PowerLab data acquisition system (PowerLab 8/30; ADInstruments) and analyzed by using LabChart 7.3.7 Pro (PowerLab; ADInstruments). Rings viability was assessed by recording the response to 0.3 μM phenylephrine. The lack of response (relaxation ≤ 10%) to the addition of 10 μM acetylcholine at the plateau of phenylephrine-induced contraction denoted the absence of a functional endothelium [48].

4.4.2. Effect of quercetin and its derivatives on phenylephrine- and high K⁺-induced contraction

Aorta rings were stimulated pharmacomechanically with 0.3 μM phenylephrine, or electromechanically with 25 mM or 60 mM KCl [49]. Once vessel tone reached a stable plateau, the drug was added cumulatively to the organ bath to assess its spasmolytic activity by constructing a concentration-response curve. At the end of these protocols, 100 μM sodium nitroprusside alone (phenylephrine-induced contraction) or 1 μM nifedipine followed by sodium nitroprusside (KCl-induced contraction) were added to prove the functional integrity of smooth muscle. The spasmolytic activity of each drug was calculated as a percentage of the maximum contraction induced by phenylephrine or KCl (taken as 100%).

4.5. Drugs and chemicals

The chemicals used included: collagenase (type XI), trypsin inhibitor, bovine serum albumin, TEA chloride, HEPES, taurine, phenylephrine, acetylcholine, quercetin, and nifedipine (Merck, Milan, Italy); sodium nitroprusside (Riedel-De Haën AG). All other substances were of analytical grade and used without further purification. Phenylephrine was solubilized in 0.1 M HCl. Nifedipine and nifedipine, dissolved directly in ethanol, and quercetin and its derivatives, dissolved directly in DMSO, were diluted at least 1000 times prior to use. Control

experiments confirmed that no response was induced in vascular preparations when DMSO or ethanol, at the final concentration used in the above dilutions (0.1%, v/v^{-1}), was added alone (data not shown). Final drug concentrations are stated in the text.

4.6. Statistical analysis

Analysis of data was accomplished by using pClamp 9.2.1.8 software (Molecular Devices Corporation) and GraphPad Prism version 5.04 (GraphPad Software Inc.). Data are reported as mean \pm s.e.m.; n is the number of cells or rings analysed (indicated in parentheses), isolated from at least three animals. Statistical analysis and significance, as measured by repeated measures ANOVA (followed by Dunnett's post hoc test), or Student's t test for unpaired samples (two tailed) were obtained using GraphPad Prism version 5.04 (GraphPad Software Inc.). In all comparisons, $P < 0.05$ was considered significant. The pharmacological response to drugs, described in terms of pEC_{50} (the $-\log$ of the EC_{50} value, i.e., the drug concentration decreasing the response by 50%), was obtained by nonlinear regression analysis.

Declaration of Competing Interest

The authors declare that they have no known competing financial interests or personal relationships that could have appeared to influence the work reported in this paper.

Acknowledgment

We wish to thank Dr. Carmelo Spinella for the assistance in some preliminary experiments. Authors from the Department of Pharmacy, Health and Nutritional Sciences – University of Calabria, and Department of Biotechnology, Chemistry and Pharmacy – University of Siena acknowledge Ministero dell'Istruzione, dell'Università e della Ricerca for grant Dipartimento di Eccellenza 2018-2022, L. 232/2016.

Appendix A. Supplementary material

Supplementary data to this article can be found online at <https://doi.org/10.1016/j.bioorg.2020.104404>.

References

- [1] H. El Gharras, Polyphenols: Food sources, properties and applications - A review, *Int. J. Food Sci. Technol.* 44 (2009) 2512–2518, <https://doi.org/10.1111/j.1365-2621.2009.02077.x>.
- [2] G. Carullo, A.R. Cappello, L. Frattaruolo, M. Badolato, B. Armentano, F. Aiello, Quercetin and derivatives: Useful tools in inflammation and pain management, *Future Med. Chem.* 9 (2017) 79–93, <https://doi.org/10.4155/fmc-2016-0186>.
- [3] S.M. Tang, X.T. Deng, J. Zhou, Q.P. Li, X.X. Ge, L. Miao, Pharmacological basis and new insights of quercetin action in respect to its anti-cancer effects, *Biomed. Pharmacother.* 121 (2020) 109604, <https://doi.org/10.1016/j.biopha.2019.109604>.
- [4] N. Polera, M. Badolato, F. Perri, G. Carullo, F. Aiello, Quercetin and its natural sources in wound healing management, *Curr. Med. Chem.* 26 (2018) 5825–5848, <https://doi.org/10.2174/0929867325666180713150626>.
- [5] G. Carullo, P. Governa, A. Leo, L. Gallelli, R. Citraro, E. Cione, M.C. Caroleo, M. Biagi, F. Aiello, F. Manetti, Quercetin-3-oleate contributes to skin wound healing targeting FFA1/GPR40, *ChemistrySelect.* 4 (2019) 8429–8433, <https://doi.org/10.1002/slct.201902572>.
- [6] G. Carullo, M. Perri, F. Manetti, F. Aiello, M.C. Caroleo, E. Cione, Quercetin-3-oleoyl derivatives as new GPR40 agonists: Molecular docking studies and functional evaluation, *Bioorganic Med. Chem. Lett.* 29 (2019) 1761–1764, <https://doi.org/10.1016/j.bmcl.2019.05.018>.
- [7] M. Badolato, G. Carullo, M. Perri, E. Cione, F. Manetti, M.L. Di Gioia, A. Brizzi, M. C. Caroleo, F. Aiello, Quercetin/oleic acid-based G-protein-coupled receptor 40 ligands as new insulin secretion modulators, *Future Med. Chem.* 9 (2017) 1873–1885, <https://doi.org/10.4155/fmc-2017-0113>.
- [8] G. D'Andrea, Quercetin: A flavonol with multifaceted therapeutic applications? *Fitoterapia* 106 (2015) 256–271, <https://doi.org/10.1016/j.fitote.2015.09.018>.
- [9] S.K. Shebeko, I.A. Zupanets, O.S. Popov, O.O. Tarasenko, A.S. Shalamay, Effects of quercetin and its combinations on health, in: *Polyphenols: Mechanisms of Action in Human Health and Disease*, Second ed., 2018, pp. 373–394, <https://doi.org/10.1016/b978-0-12-813006-3.00027-1>.
- [10] M. Kumar, E.R. Kasala, L.N. Bodduluru, V. Kumar, M. Lahkar, Molecular and biochemical evidence on the protective effects of quercetin in isoproterenol-induced acute myocardial injury in rats, *J. Biochem. Mol. Toxicol.* 31 (2017) 1–8, <https://doi.org/10.1002/jbt.21832>.
- [11] K. Arumugam, S. Thandavarayan, R.A. Arozal, W. Sari, F.R. Giridharan, V. V. Soetikno, V. Palaniyandi, S.S. Harima, M. Suzuki, K. Nagata, M. Tagaki, R. Kodama, M. Watanabe, Quercetin offers cardioprotection against progression of experimental autoimmune myocarditis by suppression of oxidative and endoplasmic reticulum stress via endothelin-1/MAPK signalling, *Free Radic. Res.* 46 (2012) 154–163, <https://doi.org/10.3109/10715762.2011.647010>.
- [12] F. Fusi, A. Trezza, M. Tramaglino, G. Sgaragli, S. Saponara, O. Spiga, The beneficial health effects of flavonoids on the cardiovascular system: Focus on K^+ channels, *Pharmacol. Res.* 152 (2020), 104625, <https://doi.org/10.1016/j.phrs.2019.104625>.
- [13] B. Eichhorn, D. Dobrev, Vascular large conductance calcium-activated potassium channels: Functional role and therapeutic potential, *Naunyn-Schmiedeberg's Arch. Pharmacol.* 376 (2007) 145–155, <https://doi.org/10.1007/s00210-007-0193-3>.
- [14] L. Shi, H. Zhang, Y. Chen, Y. Liu, N. Lu, T. Zhao, L. Zhang, Chronic exercise normalizes changes in $Ca_v1.2$ and $K_{Ca1.1}$ channels in mesenteric arteries from spontaneously hypertensive rats, *Br. J. Pharmacol.* 172 (2015) 1846–1858, <https://doi.org/10.1111/bph.13035>.
- [15] A. Perez, S. Gonzalez-Manzano, R. Jimenez, R. Perez-Abud, J.M. Haro, A. Osuna, C. Santos-Buelga, J. Duarte, F. Perez-Vizcaino, The flavonoid quercetin induces acute vasodilator effects in healthy volunteers: Correlation with beta-glucuronidase activity, *Pharmacol. Res.* 89 (2014) 11–18, <https://doi.org/10.1016/j.phrs.2014.07.005>.
- [16] D. Iozzi, R. Schubert, V.U. Kalenchuk, A. Neri, G. Sgaragli, F. Fusi, S. Saponara, Quercetin relaxes rat tail main artery partly via a PKG-mediated stimulation of $K_{Ca1.1}$ channels, *Acta Physiol.* 208 (2013) 329–339, <https://doi.org/10.1111/apha.12083>.
- [17] H.T. Zhang, Y. Wang, X.L. Deng, M.Q. Dong, L.M. Zhao, Y.W. Wang, Daidzein relaxes rat cerebral basilar artery via activation of large-conductance Ca^{2+} -activated K^+ channels in vascular smooth muscle cells, *Eur. J. Pharmacol.* 630 (2010) 100–106, <https://doi.org/10.1016/j.ejphar.2009.12.032>.
- [18] W.A. Catterall, Voltage-Gated Calcium Channels, *Cold Spring Harb. Lab.* 3 (2011), a003947.
- [19] J. Summanen, P. Vuorela, J.P. Rauha, P. Tammela, K. Marjamäki, M. Pasternack, K. Törnquist, H. Vuorela, Effects of simple aromatic compounds and flavonoids on Ca^{2+} fluxes in rat pituitary GH4C1 cells, *Eur. J. Pharmacol.* 414 (2001) 125–133, [https://doi.org/10.1016/S0014-2999\(01\)00774-9](https://doi.org/10.1016/S0014-2999(01)00774-9).
- [20] W.F. Huang, S. Ouyang, S.Y. Li, Y.F. Lin, H. Ouyang, H. Zhang, C.J. Lu, Effect of quercetin on colon contractility and L-type $Ca(2+)$ channels in colon smooth muscle of guinea-pig, *Sheng Li Xue Bao.* 61 (2009) 567–576.
- [21] S. Saponara, G. Sgaragli, F. Fusi, Quercetin as a novel activator of L-type Ca^{2+} channels in rat tail artery smooth muscle cells, *Br. J. Pharmacol.* 135 (2002) 1819–1827, <https://doi.org/10.1038/sj.bjp.0704631>.
- [22] S. Saponara, E. Carosati, P. Mugnai, G. Sgaragli, F. Fusi, The flavonoid scaffold as a template for the design of modulators of the vascular $Ca_v1.2$ channels, *Br. J. Pharmacol.* 164 (2011) 1684–1697, <https://doi.org/10.1111/j.1476-5381.2011.01476.x>.
- [23] F. Fusi, O. Spiga, A. Trezza, G. Sgaragli, S. Saponara, The surge of flavonoids as novel, fine regulators of cardiovascular Cavchannels, *Eur. J. Pharmacol.* 796 (2017) 158–174, <https://doi.org/10.1016/j.ejphar.2016.12.033>.
- [24] F. Fusi, S. Saponara, F. Pessina, B. Gorelli, G. Sgaragli, Effects of quercetin and rutin on vascular preparations: A comparison between mechanical and electrophysiological phenomena, *Eur. J. Nutr.* 42 (2003) 10–17, <https://doi.org/10.1007/s00394-003-0395-5>.
- [25] S. Saponara, G. Sgaragli, F. Fusi, Quercetin antagonism of Bay K 8644 effects on rat tail artery L-type Ca^{2+} channels, *Eur. J. Pharmacol.* 598 (2008) 75–80, <https://doi.org/10.1016/j.ejphar.2008.08.016>.
- [26] E. Fuentes, I. Palomo, Mechanisms of endothelial cell protection by hydroxycinnamic acids, *Vascul. Pharmacol.* 63 (2014) 155–161, <https://doi.org/10.1016/j.vph.2014.10.006>.
- [27] B.H. Bentzen, S.P. Olesen, L.C.B. Rønne, M. Grønnet, BK channel activators and their therapeutic perspectives, *Front. Physiol.* 5 (2014) 1–12, <https://doi.org/10.3389/fphys.2014.00389>.
- [28] G. Gessner, Y.M. Cui, Y. Otani, T. Ohwada, M. Soom, T. Hoshi, S.H. Heinemann, Molecular mechanism of pharmacological activation of BK channels, *Proc. Natl. Acad. Sci. U. S. A.* 109 (2012) 3552–3557, <https://doi.org/10.1073/pnas.1114321109>.
- [29] L. Tromba, F.M. Perla, G. Carbotta, C. Chiesa, L. Pacifico, Effect of alpha-lipoic acid supplementation on endothelial function and cardiovascular risk factors in overweight/obese youths: A double-blind, placebo-controlled randomized trial, *Nutrients.* 11 (2) (2019) 375, <https://doi.org/10.3390/nu11020375>.
- [30] G. Carullo, F. Aiello, Quercetin-3-oleate, *Molbank.* 2018 (2018) 7–10, <https://doi.org/10.3390/M1006>.
- [31] L. Biasutto, E. Marotta, U. De Marchi, M. Zoratti, C. Paradisi, Ester-based precursors to increase the bioavailability of quercetin, *J. Med. Chem.* 50 (2007) 241–253, <https://doi.org/10.1021/jm060912x>.
- [32] X. Niu, X. Qian, K.L. Magleby, Linker-gating ring complex as passive spring and Ca^{2+} -dependent machine for a voltage- and Ca^{2+} -activated potassium channel, *Neuron* 42 (2004) 745–756, <https://doi.org/10.1016/j.neuron.2004.05.001>.
- [33] A.M. Gurney, Mechanisms of Drug-induced Vasodilation, *J. Pharm. Pharmacol.* 242–251 (1994).
- [34] P. Franssen, C.E. Van Hove, A.J.A. Leloup, W. Martinet, G.R.Y. De Meyer, K. Lemmens, H. Bult, D.M. Schrijvers, Dissecting out the complex Ca^{2+} -mediated

- phenylephrine-induced contractions of mouse aortic segments, *PLoS ONE* 10 (2015) 1–17, <https://doi.org/10.1371/journal.pone.0121634>.
- [35] M.R. Koebel, G. Schmadeke, R.G. Posner, S. Sirimulla, AutoDock VinaXB: Implementation of XBSF, new empirical halogen bond scoring function, into AutoDock Vina, *J. Cheminform.* 8 (2016) 27, <https://doi.org/10.1186/s13321-016-0139-1>.
- [36] N.M. O'Boyle, M. Banck, C.A. James, C. Morley, T. Vandermeersch, G. R. Hutchison, Open Babel: An Open chemical toolbox, *J. Cheminform.* 3 (2011) 33, <https://doi.org/10.1186/1758-2946-3-33>.
- [37] G.M. Morris, H. Ruth, W. Lindstrom, M.F. Sanner, R.K. Belew, D.S. Goodsell, A. J. Olson, Software news and updates AutoDock4 and AutoDockTools4: Automated docking with selective receptor flexibility, *J. Comput. Chem.* 30 (2009) 2785–2791, <https://doi.org/10.1002/jcc.21256>.
- [38] S. Salentin, S. Schreiber, V.J. Haupt, M.F. Adasme, M. Schroeder, PLIP: Fully automated protein-ligand interaction profiler, *Nucleic Acids Res.* 43 (2015) W443–W447, <https://doi.org/10.1093/nar/gkv315>.
- [39] F. Aiello, M. Badolato, F. Pessina, C. Sticozzi, V. Maestrini, C. Aldinucci, L. Luongo, F. Guida, A. Ligresti, A. Artese, M. Allarà, G. Costa, M. Frosini, A. Schiano Moriello, L. De Petrocellis, G. Valacchi, S. Alcaro, S. Maione, V. Di Marzo, F. Corelli, A. Brizzi, Design and Synthesis of New Transient Receptor Potential Vanilloid Type-1 (TRPV1) Channel Modulators: Identification, Molecular Modeling Analysis, and Pharmacological Characterization of the N-(4-Hydroxy-3-methoxybenzyl)-4-(thiophen-2-yl)butanamide, a Sma, *ACS Chem. Neurosci.* 7 (2016) 737–748, <https://doi.org/10.1021/acschemneuro.5b00333>.
- [40] A. Mattarei, L. Biasutto, F. Rastrelli, S. Garbisa, E. Marotta, M. Zoratti, C. Paradisi, Regioselective O-derivatization of quercetin via ester intermediates. An improved synthesis of rhamnetin and development of a new mitochondriotropic derivative, *Molecules* 15 (2010) 4722–4736, <https://doi.org/10.3390/molecules15074722>.
- [41] F. Fusi, S. Saponara, G. Sgaragli, G. Cargnelli, S. Bova, Ca²⁺ entry blocking and contractility promoting actions of norbormide in single rat caudal artery myocytes, *Br. J. Pharmacol.* 137 (2002) 323–328, <https://doi.org/10.1038/sj.bjp.0704877>.
- [42] P. Mugnai, M. Durante, G. Sgaragli, S. Saponara, G. Paliuri, S. Bova, F. Fusi, L-type Ca²⁺ channel current characteristics are preserved in rat tail artery myocytes after one-day storage, *Acta Physiol.* 211 (2014) 334–345, <https://doi.org/10.1111/apha.12282>.
- [43] R. Budriesi, B. Cosimelli, P. Ioan, M.P. Ugenti, E. Carosati, M. Frosini, F. Fusi, R. Spisani, S. Saponara, G. Cruciani, E. Novellino, D. Spinelli, A. Chiarini, L-type calcium channel blockers: From diltiazem to 1,2,4-oxadiazol-5-ones via thiazinooxadiazol-3-one derivatives, *J. Med. Chem.* 52 (2009) 2352–2362, <https://doi.org/10.1021/jm801351u>.
- [44] F. Fusi, G. Sgaragli, S. Saponara, Mechanism of myricetin stimulation of vascular L-type Ca²⁺ current, *J. Pharmacol. Exp. Ther.* 313 (2005) 790–797, <https://doi.org/10.1124/jpet.104.080135>.
- [45] G.V. Petkov, F. Fusi, S. Saponara, H.S. Gagov, G.P. Sgaragli, K.K. Boev, Characterization of voltage-gated calcium currents in freshly isolated smooth muscle cells from rat tail main artery, *Acta Physiol. Scand.* 173 (2001) 257–265, <https://doi.org/10.1046/j.1365-201X.2001.00907.x>.
- [46] F. Fusi, K. Marazova, F. Pessina, B. Gorelli, M. Valoti, M. Frosini, G. Sgaragli, On the mechanisms of the antispasmodic action of some hindered phenols in rat aorta rings, *Eur. J. Pharmacol.* 394 (2000) 109–115, [https://doi.org/10.1016/S0014-2999\(00\)00152-7](https://doi.org/10.1016/S0014-2999(00)00152-7).
- [47] F. Fusi, M. Durante, G. Sgaragli, P.N. Khanh, N.T. Son, T.T. Huong, V.N. Huong, N. M. Cuong, *In vitro* vasoactivity of zerumbone from *Zingiber zerumbet*, *Planta Med.* 81 (2015) 298–304, <https://doi.org/10.1055/s-0034-1396307>.
- [48] S. Saponara, M. Durante, O. Spiga, P. Mugnai, G. Sgaragli, T. Huong, P. Khanh, N. Son, N. Cuong, F. Fusi, Functional, electrophysiological and molecular docking analysis of the modulation of Ca_v1.2 channels in rat vascular myocytes by murrayafoline A, *Br. J. Pharmacol.* 173 (2016) 292–304, <https://doi.org/10.1111/bph.13369>.
- [49] N.M. Cuong, N.T. Son, N.T. Nhan, P.N. Khanh, T.T. Huong, N.T.T. Tram, G. Sgaragli, A. Ahmed, A. Trezza, O. Spiga, F. Fusi, Vasorelaxing Activity of R (-)-3'-Hydroxy-2,4,5-trimethoxydalbergiquinol from *Dalbergia tonkinensis*: Involvement of Smooth Muscle Ca_v1.2 Channels, *Planta Med.* 86 (2020) 284–293, <https://doi.org/10.1055/a-1099-2929>.